Check for updates

FEBS Letters

FEBS PRESS science publishing by scientists

Imprinted X-chromosome inactivation impacts primitive endoderm differentiation in mouse blastocysts

Atsushi Fukuda[1,2], Nami Motosugi[1], Mikiko Ando[1], Minoru Kimura[3], Akihiro Umezawa[2] and Hidenori Akutsu[2]

1 Medical Division, Institute of Innovative Science and Technology, Tokai University, Isehara, Japan
2 Center for Regenerative Medicine, National Center for Child Health and Development, Tokyo, Japan
3 Institute of Medical Sciences, Tokai University, Isehara, Japan

Correspondence
A. Fukuda, Institute of Innovative Science and Technology, Medical Division, Tokai University, 143 Shimokasuya, Isehara, Kanagawa 259-1193, Japan
Tel: +81-463-93-1121
E-mail: fa972942@tsc.u-tokai.ac.jp
or
H. Akutsu, Center for Regenerative Medicine, National Center for Child Health and Development, 2-10-1 Okura, Setagaya, Tokyo 157-8535, Japan
Tel: +81-3-5494-7047
E-mail: akutsu-h@ncchd.go.jp

(Received 19 July 2019, revised 29 October 2019, accepted 3 November 2019, available online 25 November 2019)

doi:10.1002/1873-3468.13676

Edited by Didier Stainier

Epigenetic and transcriptome alterations are essential for lineage specification, represented by imprinted X-chromosome inactivation (iXCI) in female mouse preimplantation embryos. However, how various factors affect transcriptome states and lineage commitment remains unclear. We found that *in vitro* culture duration strongly influences transcriptional variation compared to iXCI loss. Single-cell analysis of the inner cell mass (ICM) for major transcription and epigenomic factors revealed that sex-specific differences in expression are diminished by loss of iXCI in the primitive endoderm (PrE) but not in the epiblast. Females had a higher proportion of ICM compared to that in males, and PrE development was affected by iXCI states in female embryos. Our findings provide insight into sex differences and iXCI function in lineage specification.

Keywords: imprinted X-chromosome inactivation; lineage specification; sex difference

Epigenetic dynamics and transcriptome alterations are observed after fertilization in mammals [1]. One representative epigenetic event is the establishment of X-chromosome inactivation (XCI) in female mouse embryos [2]. Generally, one of two X-chromosomes in female cells is inactivated to compensate for X-linked gene expression dosage [2]. In mice, prior to establishing XCI, the long noncoding RNA *Xist* is transcribed from the paternal X-chromosome at approximately the 4-cell stage. Parental origin-specific *Xist* expression in females leads to imprinted X-chromosome inactivation (iXCI) [3,4]. Establishment of iXCI occurs at approximately the late blastocyst stage, and hallmarks of heterochromatin such as H3K27me3 foci overlapped with *Xist* transcripts emerge [5]. Once iXCI is established, states are stably maintained during embryonic development in the primitive endoderm (PrE) and trophoblast lineages. In contrast, iXCI is reprogrammed in the epiblast [6,7]. Consequently, both female X-chromosomes are transiently present in an active state, and then, one of two X-chromosomes is randomly inactivated as differentiation proceeds.

A recent study using RNA-seq revealed that *Xist*-dependent iXCI already occurs without the H3K27me3

Abbreviations
DEGs, differentially expressed genes; ICM, inner cell mass; iXCI, imprinted X-chromosome inactivation; MAPK, mitogen-activated protein kinase; PrE, primitive endoderm; RPKM, reads per kilobase per million mapped reads; SEGs, significantly expressed genes; XCI, X-chromosome inactivation.

This is an open access article under the terms of the Creative Commons Attribution License, which permits use, distribution and reproduction in any medium, provided the original work is properly cited.

hallmark in early preimplantation phases in female mice [8]. Interestingly, the iXCI state is affected by the culture situation, and embryos produced by *in vitro* culture show an imbalanced sex ratio in birth rates [9].

During preimplantation development in mice, sex differences are observed in terms of the developmental speed by the blastocyst stage [10]. This phenotype is attributed to the presence of the Y-chromosome [10]. Moreover, the developmental competency of embryos derived from *in vivo* culture is superior to that obtained *in vitro* in mice after implantation [11]. These studies indicate that culture environment, sex differences, and iXCI impact the transcriptome and developmental propensity.

In the present study, we investigated the effects of transcriptome states by RNA-seq analysis of mouse blastocysts derived from different *in vitro* culture durations as well as following the loss of iXCI. Clustering analysis revealed that the largest clusters were formed based on culture conditions. We identified differentially expressed genes (DEGs) in sex-specific-, *in vitro* culture period-, and iXCI-dependent manner. Interestingly, upregulated genes in the female embryo derived from a short-term *in vitro* culture (*in vivo* generated embryos) compared to in the male embryo were associated with a pluripotency network. Moreover, a high-fidelity quantitative gene expression assay targeting representative transcription and epigenetic modifiers at single-cell resolution in the inner cell mass (ICM) revealed that DEGs between males and females depend on iXCI in the PrE lineage. Finally, we found that the proportion of PrE development differed between males and females, and loss of iXCI diminished the PrE differentiation potential. These findings provide insight into the relationship of iXCI with lineage specification and developmental differences based on sex.

Methods

Mouse embryo collection

Xist KO males harboring a repeat A deletion (B6.Cg-*Xist*<tm5Sado>) were a kind gift from Sado (Kindai University). *Xist* KO males (>9 weeks) were mated with 8- to 10-week-old B6D2F1 females purchased from CLEA and Sankyo Labo Service (Tokyo, Japan) *in vivo* or *in vitro* according to standard methods [3]. All animals were maintained and used in accordance with the Guidelines for the Care and Use of Laboratory Animals of the Japanese Association for Laboratory Animal Science and National Research Institute for Child Health and Development (NRICHD) and Tokai University of Japan. All animal experiments were performed according to protocols approved by the Institutional Animal Care and Use Committee of the NRICHD (Permit Number: 05–006) and Tokai University (Permit Number: 192028).

Both *in vivo* and *in vitro* fertilized embryos were cultured in KSOM (EMD Millipore, Burlington, MA, USA) until the late blastocyst stage in an atmosphere of 37 °C 5% CO_2. For *in vivo* samples, at embryonic day 2.5 (E2.5) after fertilization, embryos were flushed from the uterus using M2 medium and cultured for 2.5 days in KSOM medium until E5.0 and used for analysis. For WT embryos collection, the embryos from the littermate are used. In contrast, TYH medium [3] was used as the fertilized medium and the embryos were cultured as described above. At E5, the embryos derived from *in vitro* were used for analysis.

Single-cell isolation from ICM

Blastocysts at E5 were subjected to immune surgery to isolate the ICM using a conventional method [12]. In total, seven male, seven Xist KO female, and eight WT female embryos were used for single-cell collection. The isolated ICM was placed in 0.05% trypsin (Thermo Fisher Scientific, Waltham, MA, USA) containing 0.1% polyvinyl alcohol (PVA; Sigma, St. Louis, MO, USA) in PBS (−) and incubated for 5 min at room temperature. The trypsin-treated ICM was separated into single cells using a micromanipulator and washed with PBS (−) containing 0.1% PVA for use in the single-cell qPCR assay.

Transcriptome analysis

Total RNA was extracted using an RNeasy micro kit with DNase treatment (Qiagen, Hilden, Germany) following the manufacturer's instructions. Total RNA obtained from each sample was subjected to sequencing library construction using an Ovation Solo RNA-Seq System (NuGEN Technologies, San Carlos, CA, USA) according to the manufacturer's protocol. The Ovation SoLo RNA-Seq System integrates AnyDeplete technology for rRNA depletion and a molecular barcode system. Library quality was assessed with an Agilent 2100 Bioanalyzer High Sensitivity DNA Kit (Agilent Technologies, Santa Clara, CA, USA). The pooled libraries of the samples were sequenced using the Illumina Hiseq 1500 system (Illumina, San Diego, CA, USA) in 101-base-pair paired-end reads.

Sequencing adaptors, low-quality reads, and bases were trimmed with the Trimmomatic-0.32 tool. The sequence reads were aligned to the Mouse reference genome (mm10) using TOPHAT 2.1.1 (BOWTIE2-2.2.3, https://ccb.jhu.edu/software/tophat/index.shtml) with the option '-g 1 --no-mixed --no-discordant'. Sequence libraries of the Ovation SoLo RNA-Seq System included 8 bp molecular barcodes to detect unique RNA molecules for accurate gene expression

analysis. NUDUP tool ver.2.2 (NuGEN Technologies, San Carlos, CA, USA) was used to analyze redundancy of the molecular barcodes to identify unique molecules. Files of gene model annotations and known transcripts were downloaded from the Illumina's iGenomes website (http://support.illumina.com/sequencing/sequencing_software/igenome.html), which were necessary for whole transcriptome alignment with TOPHAT.

The aligned reads were subjected to downstream analyses using STRANDNGS 3.2 software (Agilent Technologies). The read counts allocated for each gene and transcript (RefSeq Genes 2013.04.01) were quantified using a reads per kilobase per million mapped reads (RPKM) method [13]. Genes showing a very low normalized signal value (RPKM < 1) in at least 1 sample in any group were filtered. A karyotype plot of differentially expressed genes (DEGs) was created in R 3.4 package karyoplote R version 1.4.2 [14].

Embryo sex was determined based on the expression of *Eif2s3y* mapped to the Y-chromosome. *Xist* KO females were confirmed by the absence of both *Xist* and *Eif2s3y* expression. The original data are available in GEO (GSE133845).

For pathway analysis, we used DAVID bioinformatics (https://david.ncifcrf.gov/). To identify the significantly enriched pathway based on KEGG in DAVID, Fisher's exact test ($P < 0.05$) is used to identify significant pathways.

Single-cell qPCR analysis

The isolated single cells were moved to lysis buffer using a mouth pipette under a microscope. A Single Cell-to-CT™ qRT-PCR Kit (Thermo Fisher Scientific) was used for the assay with slight modifications as described previously [15]. Briefly, half volumes of all reagents were used in the TaqMan probe assay. *Cdx2* with < 30 C_t values were considered as trophectoderm cells and removed from the analysis. C_t values > 35 were considered as no detection. Following a previous report [16] with slight modifications, we obtained single-cell expression data using qPCR. To calculate the expression levels per cell based on the C_t values, a C_t value of 30 was used as background baseline and subtracted from each C_t value. In this analysis, C_t values of no detection samples were calculated as a C_t value of 35. The resulting values were used as the normalized value for gene expression analysis.

For embryo sexing, cells in which *Eif2s3y* was detected were used as male cells, whereas other cells were used as females in WT embryos. Because we used sperm with *Xist* deletion to generate *Xist* KO embryos, cells with no *Eif2s3y* expression were regarded as *Xist* KO females. The normalized values (Log2) were used for clustering analysis with EZR (http://www.jichi.ac.jp/saitama-sct/SaitamaHP.files/statmedEN.html). To divide the cells into the epiblast or PrE lineage, the cells were classified based on the expression states of *Nanog*, *Sox2*, *Gata4*, *Gata6*, and *Sox17*, which were identified as each lineage marker. Based on the clustering results, the cells were subjected to statistical analysis (one-way analysis of variance, ANOVA, with *post hoc* test for multiple comparisons among embryo types). All TaqMan probes used in this study are shown in Table S4.

Immunofluorescence combined with DNA FISH

The zona pellucida was removed with acid Tyrode's solution (Sigma), and embryos were fixed with 2% paraformaldehyde in PBS containing 0.1% PVA (Sigma) for 20 min at room temperature and then permeabilized with 0.25% Triton X in PBS-PVA for 15 min at room temperature. After blocking with 1.5% bovine serum albumin (Sigma), the samples were incubated with primary antibodies for NANOG (1 : 200; ReproCell, Beltsville, MD, USA) and GATA4 (1 : 200; Abcam, Cambridge, UK). Alexa Fluor 488- or 546-conjugated anti-mouse or anti-rabbit IgG secondary antibodies (Thermo Fisher Scientific) were diluted with PBS-PVA and incubated with the samples for 1 h at room temperature. DNA was stained with DAPI (Vector Laboratories, Burlingame, CA, USA). Before capturing the images, the samples were attached to slide glass and covered with a cover slip. The images were observed using a LSM510 laser scanning confocal microscope (Carl Zeiss, Oberkochen, Germany), and the quantification assay was carried out using IMAGEJ software (NIH, Bethesda, MD, USA).

DNA FISH experiments were performed as described previously [17]. Briefly, after washing with PBS, the samples were incubated with PBS (−) containing RNase A for 1 h at 37 °C. The samples were treated with pepsin (Sigma) for 8–10 min, washed with PBS (−), and incubated with sexing probe (Chromosome Science Labo., Hokkaido, Japan) at 85 °C for 10 min and then incubated with 37 °C overnight. After incubation, the samples were washed as described previously [17] and images were captured.

Results

Effect of transcriptome states on culture conditions, sex, and loss of *Xist*

Mammalian embryos can develop to the late blastocyst stage *in vitro*, and blastocyst transfer into the uterus is widely used as a reproductive technique [18]. Thus, we considered that the late blastocyst is suitable for examining the effects of culture conditions, sex differences, and iXCI on transcriptome states in mice. We conducted strand-specific RNA-seq using individual late blastocysts derived from *in vivo* or *in vitro* fertilization mated with wild-type (WT) and *Xist* knockout (KO) male mice [19] and cultured *in vitro* for different durations, referred to as *in vivo* and *in vitro* samples,

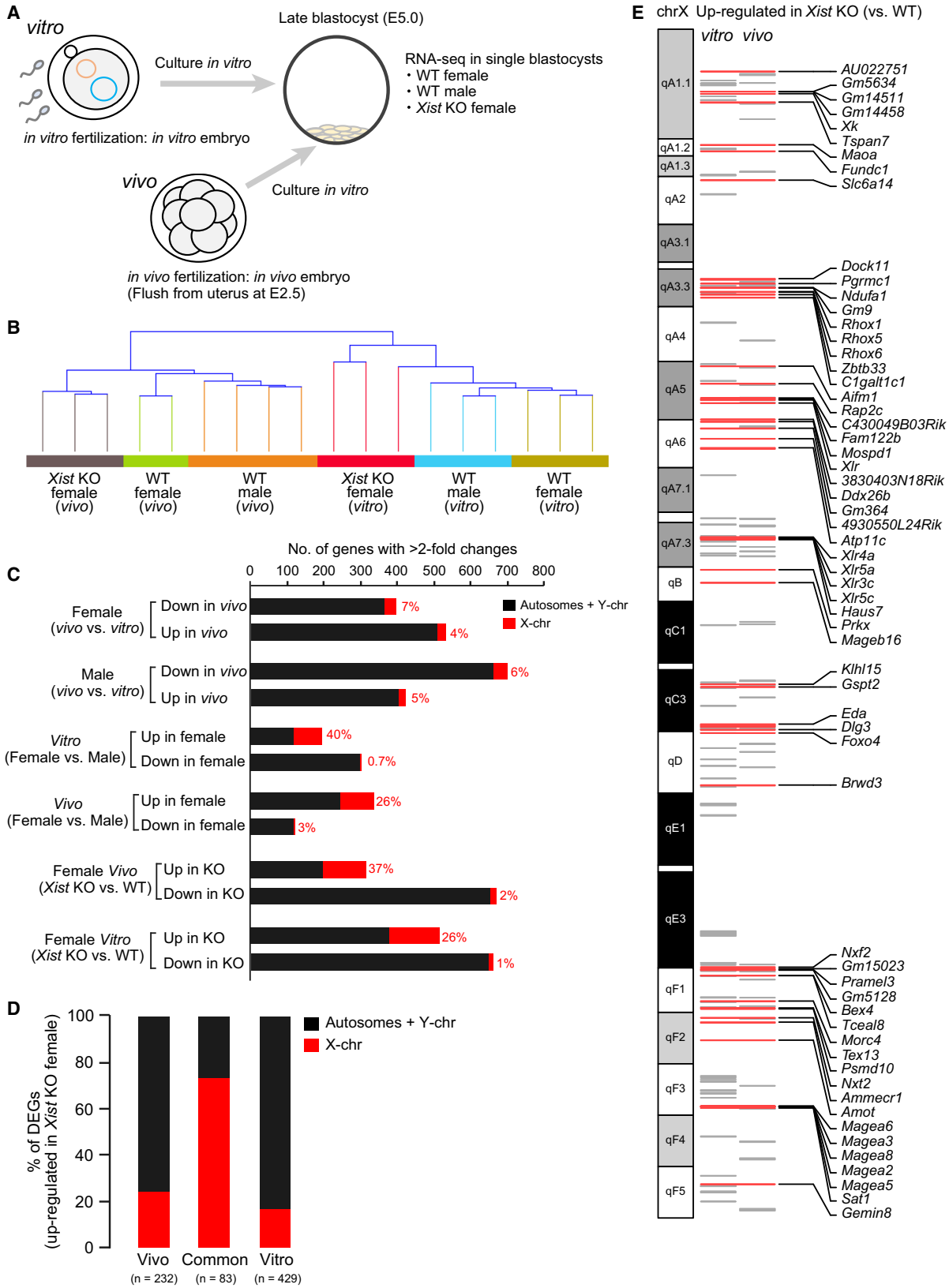

A
vitro
Late blastocyst (E5.0)
Culture in vitro
RNA-seq in single blastocysts
• WT female
• WT male
• Xist KO female
in vitro fertilization: in vitro embryo
vivo
Culture in vitro
in vivo fertilization: in vivo embryo
(Flush from uterus at E2.5)
B
Xist KO female (vivo)
WT female (vivo)
WT male (vivo)
Xist KO female (vitro)
WT male (vitro)
WT female (vitro)
C
No. of genes with >2-fold changes
0 100 200 300 400 500 600 700 800
Autosomes + Y-chr
X-chr
Female (vivo vs. vitro)
Down in vivo
Up in vivo
7%
4%
Male (vivo vs. vitro)
Down in vivo
Up in vivo
6%
5%
Vitro (Female vs. Male)
Up in female
Down in female
40%
0.7%
Vivo (Female vs. Male)
Up in female
Down in female
26%
3%
Female Vivo (Xist KO vs. WT)
Up in KO
Down in KO
37%
2%
Female Vitro (Xist KO vs. WT)
Up in KO
Down in KO
26%
1%
D
% of DEGs (up-regulated in Xist KO female)
100
80
60
40
20
0
Autosomes + Y-chr
X-chr
Vivo (n = 232)
Common (n = 83)
Vitro (n = 429)
E
chrX Up-regulated in Xist KO (vs. WT)
vitro vivo
qA1.1
qA1.2
qA1.3
qA2
qA3.1
qA3.3
qA4
qA5
qA6
qA7.1
qA7.3
qB
qC1
qC3
qD
qE1
qE3
qF1
qF2
qF3
qF4
qF5
AU022751
Gm5634
Gm14511
Gm14458
Xk
Tspan7
Maoa
Fundc1
Slc6a14
Dock11
Pgrmc1
Ndufa1
Gm9
Rhox1
Rhox5
Rhox6
Zbtb33
C1galt1c1
Aifm1
Rap2c
C430049B03Rik
Fam122b
Mospd1
Xlr
3830403N18Rik
Ddx26b
Gm364
4930550L24Rik
Atp11c
Xlr4a
Xlr5a
Xlr3c
Xlr5c
Haus7
Prkx
Mageb16
Klhl15
Gspt2
Eda
Dlg3
Foxo4
Brwd3
Nxf2
Gm15023
Pramel3
Gm5128
Bex4
Tceal8
Morc4
Tex13
Psmd10
Nxt2
Ammecr1
Amot
Magea6
Magea3
Magea8
Magea2
Magea5
Sat1
Gemin8

Fig. 1. Transcriptome states in blastocyst derived from *in vivo* and *in vitro* with *Xist* deletion. (A) Experimental scheme for RNA-seq analysis. *In vitro* samples and *in vitro* fertilized embryos were cultured until E5.0 and analyzed as *in vitro* sample. In contrast, E2.5 *in vivo* developed embryos were recovered and cultured until E5.0 and analyzed as *in vivo* samples. To generate female embryos with *Xist* deletion, males with *Xist* deletion were used for mating. (B) Hierarchical clustering analysis. Genes with RPKM (> 1 at least one group) were analyzed. (C) Number of DEGs showing more than twofold changes. (D) Proportion of up-regulated DEGs in *Xist* KO females. *In vivo*-specific, *in vitro*-specific, and commonly up-regulated genes (DEGs) were examined for chromosomal information. (E) Chromosomal distribution of up-regulated X-linked DEGs in *Xist* KO females. Red lines indicate common DEGs.

respectively (Fig. 1A). The cell numbers in blastocysts from both origins were not significantly different (Fig. S1a), indicating that the developmental stage is similar in both *in vivo* and *in vitro* embryos. The correlation coefficient among the samples was more than 0.93, exhibiting a high reproducibility (Fig. S1b). Using the genes with > 1 RPKM in at least one group, we performed hierarchical clustering analysis (Table S1). Clusters were clearly formed based on culture duration, genotype, and sex (Fig. 1B). Interestingly, the largest cluster was formed based on the *in vitro* culture duration, indicating that transcriptome states are greatly affected by the developmental environment.

To determine the gene expression states under each condition, we performed pairwise comparison and screened DEGs showing more than twofold changes (Fig. 1C and Table S2). We identified numerous DEGs in the comparison of *in vivo* and *in vitro* conditions in both male and female blastocysts, supporting the clustering results (total > 929 genes; Fig. 1C). In contrast, comparison of males and females under each condition revealed a relatively small number of DEGs (<493 genes; Fig. 1C). However, among the up-regulated genes in females compared to males, 26% (*in vivo*) and 40% (*in vitro*) were enriched in X-chromosomes (Fig. 1C). We also confirmed that X-linked genes were not dominantly expressed in this stage (Fig. S1b).

As expected, a large population of X-linked genes was up-regulated in *Xist* KO females (*in vivo*: 37% and *in vitro*: 26%; Fig. 1C), confirming the effect of *Xist*-dependent iXCI [8]. Moreover, *Xist* deletion resulted in a large number DEGs irrespective of the *in vitro* culture duration (*in vivo*: 982 genes and *in vitro*: 1172 genes; Fig. 1C).

Next, to evaluate the features of the DEGs identified in each pairwise comparison, we constructed a Venn diagram and performed KEGG pathway analysis. Several known pathways were detected in the DEGs by the comparison of *in vivo* with *in vitro* in males and females (Fig. S2a). For instance, 'Protein digestion and absorption' and 'Metabolic pathways' were commonly down- and up-regulated pathways, respectively (Fig. S2a). Interestingly, when we examined the DEGs in males and females in each culture condition, the pathway linked to 'signaling pathway regulating pluripotency of stem cell' was identified as significant (Fig. S2b). The pathway is based on the DEGs specifically up-regulated *in vivo* in females compared to *in vivo* in males (Fig. S2b). The finding that 26% (*in vivo*) and 40% (*in vitro*) of up-regulated genes in females compared to males were enriched in the X-chromosome (Fig. 1C) suggests that X-linked gene overdosage affects pluripotency networks.

In terms of the effect of *Xist* deletion, up-regulated DEGs in *Xist* KO females compared to in WT females under both culture conditions were commonly linked to 'mRNA surveillance pathway' and 'Metabolic pathway' (Fig. S2c). Although a significant pathway was not found in the up-regulated DEGs specifically in *in vivo Xist* KO females, 'p53 signaling pathway' was identified as a significant pathway in the up-regulated DEGs, specifically in *in vitro Xist* KO female embryos (Fig. S1c).

Interestingly, pluripotency-related pathway, mitogen-activated protein kinase (MAPK) signaling, and transforming growth factor-β signaling were detected as down-regulated DEGs in *Xist* KO females, specifically *in vivo* (Fig. S2c). These results indicate that although loss of iXCI causes developmental disorder in each developmental condition [19,17], the pathways influenced differ between the conditions.

These analyses were conducted with all genes, including autosomes; however, *Xist* deletion caused mainly X-linked gene overdosage (Fig. 1B). Therefore, we focused on X-linked gene expression states. Of the up-regulated DEGs in *Xist* KO females, the number of X-linked genes was high under each condition, and 73% of common DEGs were mapped to X-chromosomes (Fig. 1D). Furthermore, we found that X-linked up-regulated DEGs in the *Xist* KO female were randomly distributed over the entire X-chromosome under both culture patterns (Fig. 1E). Interestingly, among commonly up-regulated genes in *Xist* KO females, large families of *Rhox*, *Xlr*, and *Magea* were identified (Fig. 1E), suggesting that these regions might be subjected to common epigenetic regulation.

Throughout RNA-seq analysis in embryos under various conditions, we found many DEGs. In particular, many X-linked genes were up-regulated in females compared to males under both *in vivo* and *in vitro*

conditions, indicating that these conditions cause transcriptome differences between males and females. Moreover, although down-regulation of many autosomal genes was shown in Xist KO females irrespective of culture duration, *Xist*-dependent up-regulated genes on the X-chromosome were not mainly influenced by *in vitro* culture, indicating that the substantial effects of *Xist* RNA on *cis*-acting elements were stable (Fig. 1E).

Sex-specific differences in expression states of transcription and epigenetic factors depend on iXCI in the primitive endoderm but not in the epiblast

The blastocyst is the first phase of differentiation and is composed of three parts: epiblast, PrE, and trophectoderm [20]. In terms of iXCI, the state is preserved in the PrE and trophectoderm lineages but not in the epiblast [2]. Therefore, we examined how sex differences and iXCI loss impact transcription and epigenomic factors in the ICM at single-cell resolution. To investigate these intrinsic features, we used *in vivo*-derived samples for high-fidelity gene expression analysis by quantitative PCR using a TaqMan probe [3]. We confirmed that our system was highly reproducible (Fig. S3). Using this system, we collected single cells from the *in vivo*-derived ICM by immune surgery and evaluated gene expression for 72 genes related to transcription or epigenetic factors as well as XCI-related genes in male, female, and *Xist* KO female embryos (Fig. 2A). To avoid contamination and potential damage to the trophectoderm during immune surgery, we excluded the trophectoderm cells and screened cells with low expression levels of *Cdx2*, a trophectoderm maker [21], for further analysis. After removing the cells with high *Cdx2* expression, we selected 74 cells for further analysis (Table S3).

We divided the cells into two lineages, epiblast (EPI) and PrE, which are known makers for EPI (*Nanog*/*Sox2*) or PrE (*Gata4*/*Gata6*/*Sox17*) [16], to categorize the cell lineage. Hierarchical clustering analysis clearly revealed two populations based on the expression levels of these markers (Fig. 2B). Each embryo group (WT female, male, and *Xist* KO female) was randomly distributed in both the EPI and PrE groups (Fig. 2B).

Based on the clustering results, we compared the expression states in individual genes based on their origins. In EPI cells, six up-regulated genes in females were identified as significantly expressed genes (SEGs) in the comparison of WT females to males (Fig. 2C). In contrast, the comparison between WT and *Xist* KO females showed that all genes except for *Eomes* genes were not significantly expressed, indicating that the major transcription and epigenomic factors were not affected by two continuously active X-chromosomes (Fig. 2D). We also identified 12 SEGs in *Xist* KO females compared to in males, although all of them were up-regulated in *Xist* KO females (Fig. 2E). These results indicate that sex differences affect the expression levels of some types of transcription and epigenetic factors in EPI, and loss of iXCI did not affect the expression states of the analyzed genes in female embryos.

In PrE, all identified SEGs between WT females and males were up-regulated in females, as observed for EPI (Fig. 2C,F). Moreover, the identified SEGs were up-regulated in *Xist* KO females compared to in WT females, indicating that loss of iXCI leads to overexpression of the analyzed genes and X-linked genes (Fig. 2G), consistent with the results of a recent report [8]. Interestingly, comparison of *Xist* KO females and males revealed that no SEGs compared between WT females with males were significantly expressed (Fig. 2F,H), and only *Kdm5c* and *Mycn* were up-regulated in *Xist* KO females compared to males (Fig. 2H). These results indicate that female-specific genes up-regulated in PrE were affected by iXCI; however, the effect was decreased by *Xist* deletion, suggesting the dependency of PrE development.

Loss of iXCI impacts lineage specification of PrE

Next, we asked how the gene expression states affect lineage specification in the late blastocyst. We conducted immunofluorescence analysis of *NANOG* and *GATA4* following DNA-fluorescence *in situ* hybridization (FISH) using *in vivo*-derived WT female, *Xist* KO female, and male late blastocysts. As previously reported [10], we observed that the number of male cells was significantly larger than that of female cells (Fig. 3A). Interestingly, fewer *Xist* KO cells were detected compared to WT female and male cells (Fig. 3A), indicating that loss of iXCI cannot compensate for sex differences in terms of cell numbers.

Immunofluorescence analysis revealed a significantly decreased proportion of GATA4-positive cells in males compared to in WT females (6.8% in males and 9.8% in WT females; Fig. 3B,C). Moreover, a significant decrease in the GATA4-positive cell population was detected in *Xist* KO females compared to in WT females (9.8% in WT females and 5.6% in *Xist* KO females; Fig. 3B,C). Interestingly, the percentage of GATA4-positive cells in *Xist* KO females was comparable to that in males (Fig. 3B,C), supporting the quantitative PCR results.

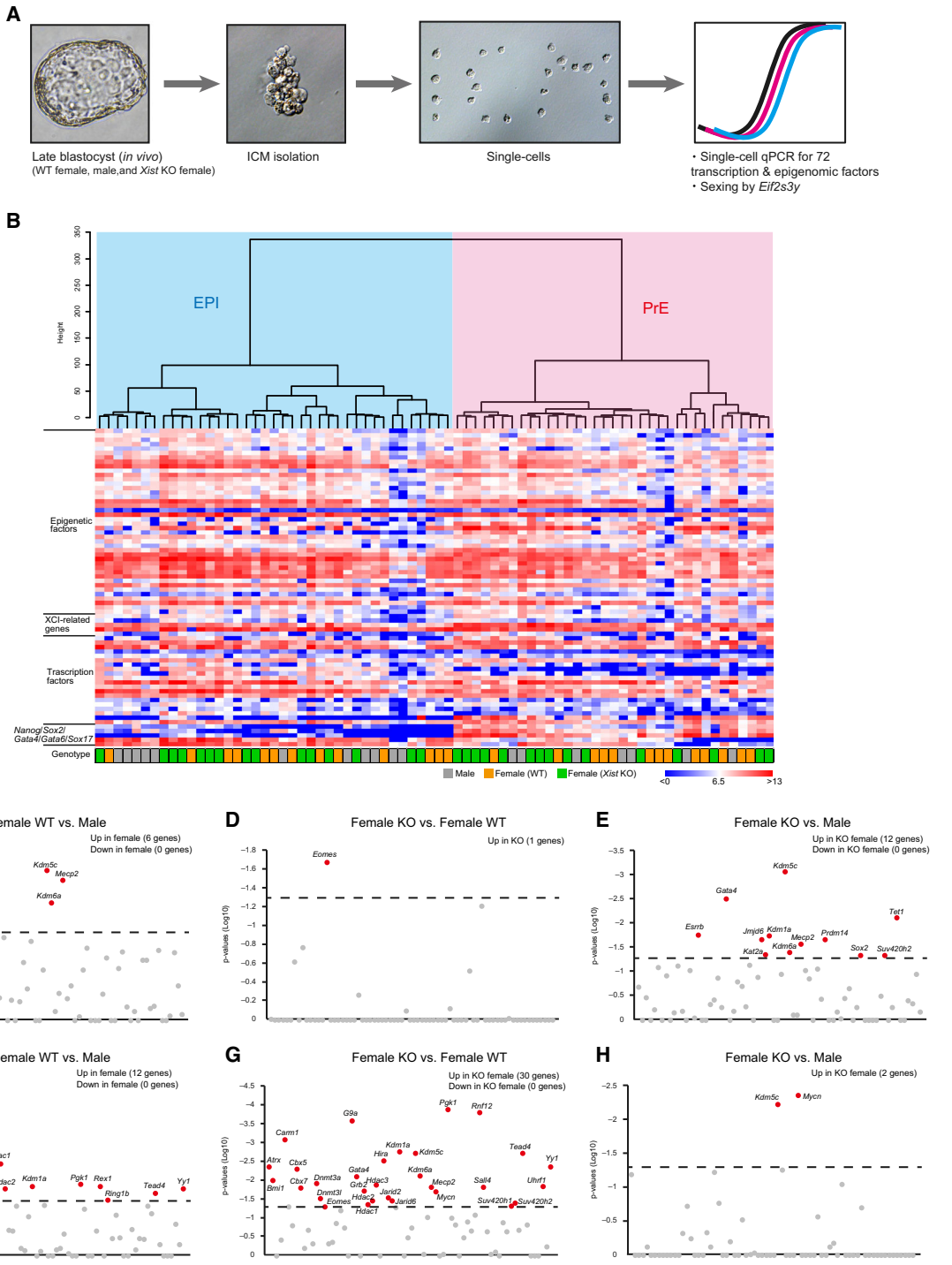


Fig. 2. Single-cell qPCR analysis in ICM. (A) Experimental scheme for single-cell analysis. The ICM was isolated from late blastocysts under the same condition of *in vivo* samples shown in Fig 1A (flushed from uterus at E2.5 and then cultured until E5.0). The single cells were analyzed by TaqMan qPCR. Sexing was based on *Eif2s3y*, which is mapped to the Y-chromosome. Cells expressing high levels of *Cdx2* were considered as trophectoderm and removed from analysis. A total of 72 genes and 74 cells were analyzed. (B) Clustering analysis based on the expression levels of *Nanog* (EPI), *Sox2* (EPI), *Gata4* (PrE), *Gata6* (PrE), and *Sox17* (PrE). The cells were categorized into the EPI and PrE lineages based on the expression levels of these markers. Heat map showing the expression levels of each sample. (C–E) SEGs in EPI lineage. (F–H) SEGs in PrE lineage. For pairwise comparison in each group, the average expression levels in each group were used and one-way ANOVA was applied to determine significance ($P < 0.05$). SEGs with a *P*-value less than < 0.05 are shown in red.

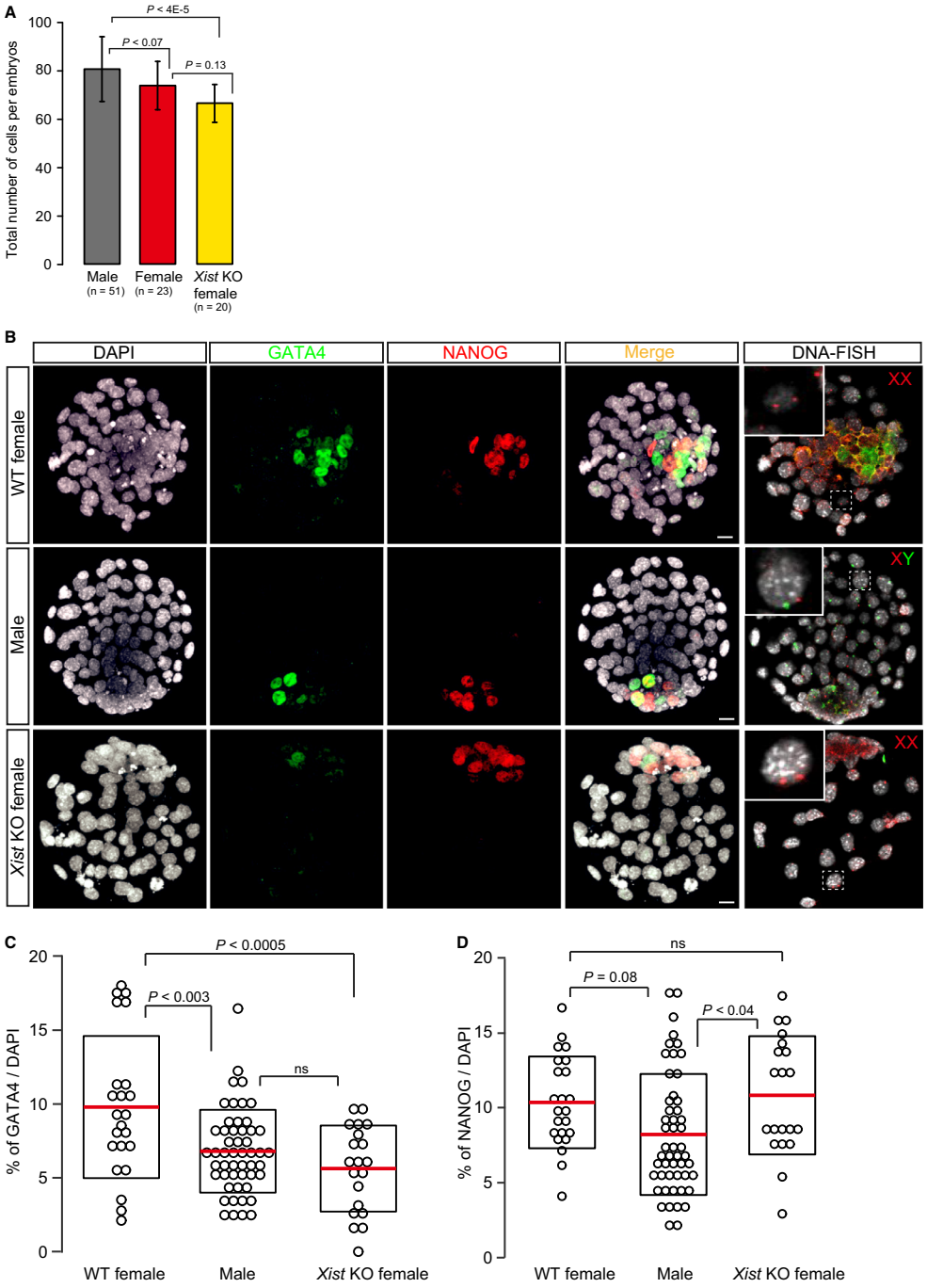


Fig. 3. Loss of iXCI impacts lineage specification. (A) Cell number analysis in each genotype at late blastocyst. DAPI-stained nuclei were counted to determine cell number. *n* is the number of embryos analyzed. One-way ANOVA was used for statistical calculations. (B) Immunofluorescence analysis of NANOG and GATA4 following DNA FISH. Representative images are shown. For DNA FISH, sex chromosomes were used for sex determination. (C, D) Quantification of GATA4- (C) and NANOG-positive (D) cells. Each dot indicates an analyzed embryo. One-way ANOVA was used for statistical calculation. The scale bar indicates 10 μm.

In contrast, the percentage of *NANOG*-positive cells was decreased only in male embryos (males: 8.2%, WT females 10.3%, and *Xist* KO female: 10.8%; Fig. 3A,C). Furthermore, the single blastocyst RNA-seq data in PrE and EPI markers also showed that expression levels of *Nanog*, *Sox2*, *Sox17*, and *Gata4* in

females were higher than those in males (Fig. S4a). Given that the proportions of GATA4- and NANOG-positive cells of female embryos were higher than those of males and the CDX2-positive cell proportion is higher in males than in females (Fig. 3C,D and Fig. S4b), male embryos developed the trophectoderm lineage well compared with females.

Taken together, these results indicate that sex differences occur in both EPI and PrE lineage development. Particularly, iXCI impacts on PrE lineage specification in females.

Discussion

Transcriptome analysis revealed that culture conditions greatly impact gene expression states and *Xist* deletion. Given that the developmental competency of embryos derived from *in vitro* fertilized and culture is inferior to *in vivo* embryos [11], the identified pathways may be responsible for the poor development in *in vitro*-derived embryos. For example, the Wnt, MAPK, and vascular endothelial growth factor pathways were identified as commonly up-regulated in *in vitro*-derived male and female embryos (Fig. S1a). Because these pathways have been widely studied and small molecules are used for their repression [22], transient treatment during *in vitro* culture may have beneficial effects on development.

Because we observed that up-regulated genes in WT females compared to in males were enriched on the X-chromosome, sex differences in transcriptome would be caused by X-chromosome reactivation in the female epiblast [2]. Interestingly, we found that pathways linked to pluripotency were induced by up-regulated genes in female embryos *in vivo* compared to males (Fig. S1b). Recent studies using mouse embryonic stem cells indicated that having two active X-chromosomes blocks differentiation via *Dusp9*-mediated MAPK pathway suppression [23,24]. Consistent with the results of stem cell studies, *Dusp9* was up-regulated in female embryos compared to male embryos (Table S1). Collectively, overexpression of X-linked genes was associated with pluripotent states and responsible for the high population of *NANOG*-positive cells in female compared to male embryos and in *Xist* KO females (Fig. 3D).

In terms of the effect of *Xist* deletion on the transcriptome, up-regulation of the *Rhox* and *Magea* families in *Xist* KO female is consistent with the results described in previous studies [8]. Importantly, overexpression of *Rhox5* in mouse embryonic stem cells impairs the differentiation potential [25], indicating that dysregulation of *Rhox*-family genes is one factor responsible for the developmental disorder in *Xist* deletion. In contrast, although the results for the *Xlr* family have not been reported in *Xist* dependency in preimplantation embryos, given that the *Xlr*, *Magea*, and *Rhox* families are under the control of H3K9me2 [26,27] and *Xist* RNA overlaps with H3K9me2 [28], the results showing the *Xist* dependency of these families are reasonable.

Single-cell analysis showed that the number of SEGs in the comparison between males and *Xist* KO females was greater than that between in males and WT females (Fig. 2C,E). Although the exact reason for the difference remains unclear, and given that paternal X-chromosome reactivation occurs transiently in WT females [6,7] and RNA-seq analysis identified many DEGs between WT and Xist KO female embryos (Fig. 1C), the results suggest that EPI cells in *Xist* KO females are not exactly the same as those in WT females. Moreover, among of the up-regulated genes in *Xist* KO females compared with males, *Sox2* and *Esrrb* were identified as SEGs [29,30]. As both genes are known as pluripotency-related genes, a defect to exit to pluripotency observed in female embryonic stem cells [23] may also occur in *Xist* KO female epiblasts.

In contrast, analysis of the PrE lineage revealed that that most transcriptional and epigenomic factors analyzed in this study were up-regulated in *Xist* KO female cells compared to WT female cells. These results are consistent with the genome-wide scale of transcriptional states in *Xist* KO trophoblasts [31]. Although the mechanisms underlying the up-regulation of X-linked genes and autosomal genes by loss of iXCI remain unknown, many transcription and epigenetic factors are mapped to X-chromosome such as *Atrx* and *Mecp2*. Indeed, *Mecp2* is highly up-regulated in PrE and *Xist* KO female embryos and plays an important role in gene silencing [32]. Therefore, multiple derepression of gene silencers mapped to the X-chromosome may cause genome-wide up-regulation of autosomal genes.

Finally, in terms of ICM development, we found that PrE development in *Xist* KO female embryos was similar to that in males, supported by the single-cell qPCR results. Poor development of PrE in *Xist* KO female embryos was previously observed when *SOX17*-positive cells were reduced [8]. In contrast to PrE development, we found no differences in EPI development in *Xist* KO females compared to WT females. Although the inactive X-chromosome is reactivated in EPI [2], *Xist*-dependent X-linked gene silencing occurs before X-chromosome reactivation [8,17]. Thus, these results indicate that having both X-chromosomes continuously active is dispensable for EPI specification in blastocysts.

In conclusion, sex differences exist during early embryonic development in mice, and ICM development differs between males and females. In female embryos, iXCI impacts PrE development, revealing a novel role for iXCI in lineage specification.

Acknowledgements

We would like to thank Prof T. Sado (Kindai University) for gifting *Xist* KO mice and helpful comment, Prof H. Kobayashi (Tokai University) for discussion, and A. Mitani and A. Nakamura for their technical assistance. We also thank Dr Kikugawa (DNA Chip Research Inc.) for bioinformatic analysis and are grateful to Dr C. Okada, the Support Center for Medical Research and Education, Tokai University. This research was supported by AMED under Grant Number JP19bm0704038 to AF and Grants-in-Aid for Scientific Research (A) (17H01588) to HA.

Author contributions

AF conceived and designed the study. AF conducted most of experiments and analyzed the data with help from NM, MA, and MK. AF, AU, and HA supervised the study. AF wrote the manuscript with input from all of co-authors.

References

1 Burton A and Torres-Padilla ME (2014) Chromatin dynamics in the regulation of cell fate allocation during early embryogenesis. *Nat Rev Mol Cell Biol* **15**, 723–734.
2 Augui S, Nora EP and Heard E (2011) Regulation of X-chromosome inactivation by the X-inactivation centre. *Nat Rev Genet* **12**, 429–442.
3 Fukuda A, Tomikawa J, Miura T, Hata K, Nakabayashi K, Eggan K, Akutsu H and Umezawa A (2014) The role of maternal-specific H3K9me3 modification in establishing imprinted X-chromosome inactivation and embryogenesis in mice. *Nat Commun* **5**, 5464.
4 Takagi N and Sasaki M (1975) Preferential inactivation of the paternally derived X chromosome in the extraembryonic membranes of the mouse. *Nature* **256**, 640–642.
5 Plath K, Fang J, Mlynarczyk-Evans SK, Cao R, Worringer KA, Wang H, de la Cruz CC, Otte AP, Panning B and Zhang Y (2003) Role of histone H3 lysine 27 methylation in X inactivation. *Science* **300**, 131–135.
6 Okamoto I, Otte AP, Allis CD, Reinberg D and Heard E (2004) Epigenetic dynamics of imprinted X inactivation during early mouse development. *Science* **303**, 644–649.
7 Mak W, Nesterova TB, de Napoles M, Appanah R, Yamanaka S, Otte AP and Brockdorff N (2004) Reactivation of the paternal X chromosome in early mouse embryos. *Science* **303**, 666–669.
8 Borensztein M, Syx L, Ancelin K, Diabangouaya P, Picard C, Liu T, Liang JB, Vassilev I, Galupa R, Servant N *et al.* (2017) Xist-dependent imprinted X inactivation and the early developmental consequences of its failure. *Nat Struct Mol Biol* **24**, 226–233.
9 Tan K, An L, Miao K, Ren L, Hou Z, Tao L, Zhang Z, Wang X, Xia W, Liu J *et al.* (2016) Impaired imprinted X chromosome inactivation is responsible for the skewed sex ratio following in vitro fertilization. *Proc Natl Acad Sci USA* **113**, 3197–3202.
10 Burgoyne PS (1993) A Y-chromosomal effect on blastocyst cell number in mice. *Development* **117**, 341–345.
11 Delle Piane L, Lin W, Liu X, Donjacour A, Minasi P, Revelli A, Maltepe E and Rinaudo PF (2010) Effect of the method of conception and embryo transfer procedure on mid-gestation placenta and fetal development in an IVF mouse model. *Hum Reprod* **25**, 2039–2046.
12 Nagy A, Gertsenstein M, Vintersten K and Behringer R (2006) Immunosurgery: isolating the inner cell mass (ICM) of blastocysts. *CSH Protoc* **2006**.
13 Mortazavi A, Williams BA, McCue K, Schaeffer L and Wold B (2008) Mapping and quantifying mammalian transcriptomes by RNA-Seq. *Nat Methods* **5**, 621–628.
14 Gel B and Serra E (2017) karyoploteR: an R/Bioconductor package to plot customizable genomes displaying arbitrary data. *Bioinformatics* **33**, 3088–3090.
15 Fukuda A, Mitani A, Miyashita T, Umezawa A and Akutsu H (2015) Chromatin condensation of Xist genomic loci during oogenesis in mice. *Development* **142**, 4049–4055.
16 Guo G, Huss M, Tong GQ, Wang C, Li Sun L, Clarke ND and Robson P (2010) Resolution of cell fate decisions revealed by single-cell gene expression analysis from zygote to blastocyst. *Dev Cell* **18**, 675–685.
17 Fukuda A, Mitani A, Miyashita T, Sado T, Umezawa A and Akutsu H (2016) Maintenance of Xist imprinting depends on chromatin condensation state and Rnf12 dosage in mice. *PLoS Genet* **12**, e1006375.
18 Gardner DK, Schoolcraft WB, Wagley L, Schlenker T, Stevens J and Hesla J (1998) A prospective randomized trial of blastocyst culture and transfer in in-vitro fertilization. *Hum Reprod* **13**, 3434–3440.
19 Hoki Y, Kimura N, Kanbayashi M, Amakawa Y, Ohhata T, Sasaki H and Sado T (2009) A proximal conserved repeat in the Xist gene is essential as a genomic element for X-inactivation in mouse. *Development* **136**, 139–146.

20 Chazaud C and Yamanaka Y (2016) Lineage specification in the mouse preimplantation embryo. *Development* **143**, 1063–1074.
21 Strumpf D, Mao CA, Yamanaka Y, Ralston A, Chawengsaksophak K, Beck F and Rossant J (2005) Cdx2 is required for correct cell fate specification and differentiation of trophectoderm in the mouse blastocyst. *Development* **132**, 2093–2102.
22 Weinberger L, Ayyash M, Novershtern N and Hanna JH (2016) Dynamic stem cell states: naive to primed pluripotency in rodents and humans. *Nat Rev Mol Cell Biol* **17**, 155–169.
23 Schulz EG, Meisig J, Nakamura T, Okamoto I, Sieber A, Picard C, Borensztein M, Saitou M, Bluthgen N and Heard E (2014) The two active X chromosomes in female ESCs block exit from the pluripotent state by modulating the ESC signaling network. *Cell Stem Cell* **14**, 203–216.
24 Choi J, Clement K, Huebner AJ, Webster J, Rose CM, Brumbaugh J, Walsh RM, Lee S, Savol A, Etchegaray JP *et al.* (2017) DUSP9 modulates DNA hypomethylation in female mouse pluripotent stem cells. *Cell Stem Cell* **20**, 706–719.e7.
25 Fan Y, Melhem MF and Chaillet JR (1999) Forced expression of the homeobox-containing gene Pem blocks differentiation of embryonic stem cells. *Dev Biol* **210**, 481–496.
26 Auclair G, Borgel J, Sanz LA, Vallet J, Guibert S, Dumas M, Cavelier P, Girardot M, Forne T, Feil R *et al.* (2016) EHMT2 directs DNA methylation for efficient gene silencing in mouse embryos. *Genome Res* **26**, 192–202.
27 Wen B, Wu H, Shinkai Y, Irizarry RA and Feinberg AP (2009) Large histone H3 lysine 9 dimethylated chromatin blocks distinguish differentiated from embryonic stem cells. *Nat Genet* **41**, 246–250.
28 Escamilla-Del-Arenal M, da Rocha ST, Spruijt CG, Masui O, Renaud O, Smits AH, Margueron R, Vermeulen M and Heard E (2013) Cdyl, a new partner of the inactive X chromosome and potential reader of H3K27me3 and H3K9me2. *Mol Cell Biol* **33**, 5005–5020.
29 Masui S, Nakatake Y, Toyooka Y, Shimosato D, Yagi R, Takahashi K, Okochi H, Okuda A, Matoba R, Sharov AA *et al.* (2007) Pluripotency governed by Sox2 via regulation of Oct3/4 expression in mouse embryonic stem cells. *Nat Cell Biol* **9**, 625–635.
30 van den Berg DL, Zhang W, Yates A, Engelen E, Takacs K, Bezstarosti K, Demmers J, Chambers I and Poot RA (2008) Estrogen-related receptor beta interacts with Oct4 to positively regulate Nanog gene expression. *Mol Cell Biol* **28**, 5986–5995.
31 Sakata Y, Nagao K, Hoki Y, Sasaki H, Obuse C and Sado T (2017) Defects in dosage compensation impact global gene regulation in the mouse trophoblast. *Development* **144**, 2784–2797.
32 Jones PL, Veenstra GJ, Wade PA, Vermaak D, Kass SU, Landsberger N, Strouboulis J and Wolffe AP (1998) Methylated DNA and MeCP2 recruit histone deacetylase to repress transcription. *Nat Genet* **19**, 187–191.

Supporting information

Additional supporting information may be found online in the Supporting Information section at the end of the article.

Fig. S1. Characterization of samples for RNA-seq analysis.
Fig. S2. Venn diagram and KEGG pathway analysis.
Fig. S3. Effect of preamplification on qPCR assay.
Fig. S4. Expression states of lineage markers.
Table S1. RNA-seq data with more than 1 RPKM.
Table S2. Differentially expressed gene lists.
Table S3. Single qPCR data.
Table S4. TaqMan probe information.